Computation of the asymptotic states of modulated open quantum systems with a numerically exact realization of the quantum trajectory method

V. Volokitin,[1] A. Liniov,[1] I. Meyerov,[1] M. Hartmann,[2] M. Ivanchenko,[3] P. Hänggi,[2] and S. Denisov[2,3]

[1]*Mathematical Software and Supercomputing Technologies Department, Lobachevsky State University of Nizhny Novgorod, Russia*

[2]*Institut für Physik, Universität Augsburg, Universitätsstraße 1, D-86135 Augsburg, Germany*

[3]*Department of Applied Mathematics, Lobachevsky State University of Nizhny Novgorod, Russia*

(Received 12 October 2017; published 29 November 2017)

Quantum systems out of equilibrium are presently a subject of active research, both in theoretical and experimental domains. In this work, we consider time-periodically modulated quantum systems that are in contact with a stationary environment. Within the framework of a quantum master equation, the asymptotic states of such systems are described by time-periodic density operators. Resolution of these operators constitutes a nontrivial computational task. Approaches based on spectral and iterative methods are restricted to systems with the dimension of the hosting Hilbert space $\dim\mathcal{H} = N \lesssim 300$, while the direct long-time numerical integration of the master equation becomes increasingly problematic for $N \gtrsim 400$, especially when the coupling to the environment is weak. To go beyond this limit, we use the quantum trajectory method, which unravels the master equation for the density operator into a set of stochastic processes for wave functions. The asymptotic density matrix is calculated by performing a statistical sampling over the ensemble of quantum trajectories, preceded by a long transient propagation. We follow the ideology of event-driven programming and construct a new algorithmic realization of the method. The algorithm is computationally efficient, allowing for long "leaps" forward in time. It is also numerically exact, in the sense that, being given the list of uniformly distributed (on the unit interval) random numbers, $\{\eta_1,\eta_2,...,\eta_n\}$, one could propagate a quantum trajectory (with η_i's as norm thresholds) in a numerically exact way. By using a scalable N-particle quantum model, we demonstrate that the algorithm allows us to resolve the asymptotic density operator of the model system with $N = 2000$ states on a regular-size computer cluster, thus reaching the scale on which numerical studies of modulated Hamiltonian systems are currently performed.

DOI: 10.1103/PhysRevE.96.053313

I. INTRODUCTION

Most of *in vivo* quantum systems are interacting with an environment. Although often weak, this interaction becomes relevant when studying the evolution of a system over long time scales. In particular, the asymptotic state of such an *open* system depends both on the unitary action induced by the system Hamiltonian, and the action of the environment, conventionally termed "dissipation." A recent concept of "engineering by dissipation" [1–7], i.e., the creation of designated pure and highly entangled states of many-body quantum systems by using specially designed dissipative operators, has promoted the role of quantum dissipation to the same level of importance as unitary evolution.

The use of time-periodic modulations constitutes another means to manipulate the states of a quantum system. In the coherent limit, when the system is decoupled from the environment, the modulations imply an explicit time-periodicity of the system Hamiltonian, $H(t+T) = H(t)$. The dynamics of the system are determined by the basis of time-periodic *Floquet eigenstates* [8–10,12]. The properties of the Floquet states depend on various modulation parameters. Modulations being resonant with intrinsic system frequencies may create a set of nonequilibrium eigenstates with properties drastically different from those of time-independent Hamiltonians. Modulations enrich the physics occurring in fields such as quantum optics, optomechanics, solid state, and ultra-cold atom physics [10–13] and disclose a whole spectrum of new phenomena [14–18].

What are the possible physical prospects of a synergy between environment-induced decoherence and periodic modulations when both aspects impact a N-state quantum system? Of course, this question should be rephrased more precisely, depending on the context of the problem. However, we are confident that a partial answer to this question, even in its most general form, will be appreciated by several communities working on many-body localization (MBL) [19–23], Floquet topological insulators [15], and dissipative engineering [1,4,5].

There exist several approaches to address the evolution of open quantum systems [24]. A popular (especially in the context of quantum optics [25]) approach is based on the quantum master equation with the generator $\mathcal{L}$ of the Lindblad form [26,27] (we set $\hbar = 1$):

$$\begin{aligned}\dot{\varrho} &= \mathcal{L}(\varrho) = -i[H(t),\varrho] + \sum_{k=1}^{K} \gamma_k(t)\cdot\mathcal{D}_k(\varrho),\\ \mathcal{D}_k(\varrho) &= V_k\varrho V_k^\dagger - \frac{1}{2}\{V_k^\dagger V_k,\varrho\}.\end{aligned} \tag{1}$$

Here, ϱ denotes the system density matrix, while the set of quantum jump operators, V_k, $k = 1,...,K$, capture the action of the environment on the system. The jump operators act on the coherent system dynamics via K "channels" with time-dependent rates $\gamma_k(t)$. Finally, $[\cdot,\cdot]$ and $\{\cdot,\cdot\}$ denote the commutator and the anticommutator, respectively.

As an object of mathematical physics, Eq. (1) exhibits a specifically tailored structure and possesses a variety of important properties [27]. In the case of a time-independent,

stationary Hamiltonian $H(t) \equiv H$, the generator $\mathcal{L}$ induces a continuous set of completely positive quantum maps $\mathcal{P}_t = e^{\mathcal{L}t}$. Under some conditions, the system evolves from an initial state ϱ^{init} toward a unique and time-independent asymptotic state ϱ^{eq}, $\lim_{t\to\infty} \mathcal{P}_t \varrho^{\text{init}} = \varrho^{\text{eq}}$ [27]. When time-periodic modulations are present, Eq. (1) preserves the complete positivity of the time evolution if all those coupling rates are nonnegative at any instance of time, $\gamma_k(t) \geqslant 0$, $\forall t$ [27]. Under certain, experimentally relevant assumptions, an approximation in terms of a "time-dependent Hamiltonian and a time-independent dissipation" provides a suitable approximation [27].

Here, we address the particular case of quenchlike, periodic modulations of period T with the time-periodic dependence of the Hamiltonian $H(t)$, $t \in [0,T]$, consisting of a switch between several constant Hamiltonians. A common choice is a setup composed of two Hamiltonians,

$$H(t) = \begin{cases} H_1, & \text{for} \quad 0 \leq t \bmod T < \tau \\ H_2, & \text{for} \quad \tau \leq t \bmod T < T \end{cases}, \tag{2}$$

with $\tau \in [0,T]$. This minimal form has recently been used to investigate the connection between integrability and thermalization [21,28,29] or, similarly, for disorder-induced localization [20] in *coherent* periodically modulated many-body systems.

From a mathematical point of view, Eqs. (1) and (2) define a linear equation with a time-periodic generator $\mathcal{L}(t)$. Therefore, Floquet theory applies and asymptotic solutions of the equation are time-periodic with temporal period T [10,30]. $\mathcal{L}(t)$ is a dissipative operator and, in the absence of relevant symmetries, the system evolution in the asymptotic limit $t \to \infty$ is determined by a unique "quantum attractor," i.e., by an asymptotic, time-periodic density operator obeying $\varrho^{\text{att}}(\tau + nT) = \varrho^{\text{att}}(\tau)$, $\tau \in [0,T]$ and $n \in \mathbb{Z}^+$. The main objective here consists in explicit numerical evaluation of the matrix form of this operator.

To use spectral methods (complete or partial diagonalization and different kinds of iterative algorithms [31]) to calculate ϱ^{att} as an eigenelement of the corresponding Floquet map $\mathcal{P}(T) = e^{\mathcal{L}_2(T-\tau)} e^{\mathcal{L}_1 \tau}$ would imply that one has to deal with N^2 computationally expensive operations. In the case of periodically modulated systems it restricts the use of spectral methods to $N \lesssim 300$ [32].

A direct propagation of Eq. (1) for a time span long enough for $\varrho(t)$ to approach the quantum attractor is not feasible for $N \gtrsim 400$ for at least two reasons: Direct propagation requires to numerically propagate $N^2 \gtrsim 1.6 \times 10^5$ complex differential equations with time-dependent coefficients, so that the accuracy might become problematic for large evolution times. Although the accuracy may be improved by implementing high(er)-order integration schemes [33] or Faber and Newton polynomial integrators [34], this approach is hardly parallelizable so one could not benefit by propagating equations on a cluster [35].

Systems containing $N = 400$ states may still be too small, for example, to explore MBL effects in open periodically-modulated systems. Is it possible to exceed this limit? If so, to what extent is this feasible? We attempt to answer these two questions by first unraveling of the quantum master Eq. (1) into a set of stochastic realizations, by resorting to the celebrated method of "quantum trajectories" [36–39]. This method allows one to transform the problem of the numerical solution of Eqs. (1) and (2) into a task of statistical sampling over quantum trajectories which form vectors of the size N. The price to be paid for the reduction from N^2 to N is that we now have to sample over many realizations. This problem is very well suited for parallelization and we thus can benefit from the use of a computer cluster. If the number of realizations M_r becomes large, the sampling of the density operator $\varrho(t)$ with the initial condition $\varrho^{\text{init}} = |\psi^{\text{init}}\rangle\langle\psi^{\text{init}}|$ converges to the solution of Eq. (1) [36,37] provided that the propagation of the trajectories was performed in a *numerically exact way* (we discuss the precise meaning of this in Sec. III).

We address the generic system, specified by Eqs. (1) and (2), with no conditions imposed on the operators $H(t)$ and V_k (for example, they need not be local [40,41] and with no *a priori* knowledge of the attractor state. There are two important issues. First is the time t_p after which the trajectories are sampled. To guarantee that the asymptotic regime is reached, this time has to exceed the longest relaxation time scale of the system. Practically, this means that the sampling over trajectories started at time $t_p = ST$, with integer $S \gg 1$, does converge to a density operator, which is close to the asymptotic $\varrho^{\text{att}}(\tau = 0)$. Second, to minimize numerical errors due to long propagation, we devise an integration scheme based on a set of exponential propagators. For quenchlike periodic modulations this implies a finite number of propagators, which can be precalculated and stored locally on each cluster node, as we discuss in the next section.

For a scalable model, a periodically rocked and dissipative system of $N - 1$ interacting bosons, we find that the statistical variance of the sampling does not grow infinitely with t_p but rather saturates to a limit-cycle evolution. Therefore, the number of trajectories $M_r(\epsilon)$ needed to estimate elements of ϱ^{att} with accuracy ϵ (defined with some matrix norm), remains finite. Assuming that the propagation can be performed for an arbitrary large time t_p with required accuracy, we are left with the only problem to sample over a sufficiently large number of trajectories.

In addition, in the asymptotic limit, the sampling of $\varrho^{\text{att}}(\tau = 0)$ can be performed over individual trajectories stroboscopically, after each period T. This increases the efficiency of sampling via the use of the same trajectory without having to initiate yet a new trajectory and then propagating it up to time t_p. Our results confirm that by implementing this approach on a cluster, it is possible to resolve attractors of periodically modulated open systems with several thousand quantum states, thus increasing N by one order of magnitude.

The present work is organized as follows: In Sec. II we outline the method of quantum trajectories and describe the algorithmic realization of the method. Statistical aspects of sampling are briefly discussed in Sec. III. In Sec. IV we introduce a scalable model system, which serves as a test bed for the algorithm. Section V is devoted to the implementation of the algorithm on a cluster together with an analysis of its performance and scalability. Section VI reports numerical results obtained for the test case. The findings of the study are summarized together with an outline of further perspectives in Sec. VII.

II. QUANTUM TRAJECTORY AS AN EVENT-DRIVEN PROCESS

To sample the solution of Eqs. (1) and (2) up to some time t_p using quantum trajectories (also known under the labels of quantum jump method [38] or the Monte Carlo wave function method [37]) we first have to calculate the effective non-Hermitian Hamiltonian,

$$\tilde{H}(t) = H(t) - \frac{i}{2}\sum_{k=1}^{K} V_k^\dagger V_k, \tag{3}$$

and then proceed along the following path of instructions [36]:

(1) initiate the trajectory in a pure state $|\psi^{\text{init}}\rangle$;

(2) draw a random number η which is uniformly distributed on the unit interval;

(3) propagate the quantum state $|\psi(t)\rangle$ in time using the effective Hamiltonian $\tilde{H}(t)$;

(4) the squared norm $\||\psi(t)\rangle\|^2$ decays monotonically. When the equality $\eta = \||\psi(t)\rangle\|^2$ is reached, stop the propagation and normalize the state vector, $|\psi(t)\rangle \to |\psi(t)\rangle/\||\psi(t)\rangle\|$;

(5) perform a quantum jump: select the jump operator D_k with probability $p_k = \gamma_k\|D_k|\psi(t)\rangle\|^2/\sum_{k=1}^{K}\gamma_k\|D_k|\psi(t)\rangle\|^2$ and apply the transformation $|\psi(t)\rangle \to D_k|\psi(t)\rangle/\|D_k|\psi(t)\rangle\|$;

(6) repeat steps 2–5 until the desired time t_p is reached.

The density matrix can then be sampled from a set of M_r realizations as $\varrho(t_p;M_r) = \frac{1}{M_r}\sum_{j=1}^{M_r}|\psi_j(t_p)\rangle\langle\psi_j(t_p)|$. Formally, in the limit $M_r \to \infty$, the result $\varrho(t_p;M_r)$ converges towards the solution of Eq. (1) at time t_p for the given initial density matrix $\varrho^{\text{init}} = |\psi^{\text{init}}\rangle\langle\psi^{\text{init}}|$ [24,36]. The density matrix can also be sampled at any other instance of time $t \in [0,t_p]$. This does not affect the propagation of the trajectory and only demands normalization of the state vector $|\psi(t)\rangle$ before updating $\varrho(t;M_r) \to \varrho(t;M_r+1)$. More specifically, an element of the density matrix, $\varrho_{ls}(t)$, should be sampled as

$$\varrho_{ls}(t;M_r) = \frac{1}{M_r}\sum_{j=1}^{M_r} c_{j,l}(t)c_{j,s}^*(t), \tag{4}$$

where $c_{j,l}(t)$ is the lth coefficient of the expansion (in the same basis $\{|\psi_j(t)\rangle\}, k = 1,\ldots,N$ used to express the density matrix) of the normalized wave-function, $|\psi_j(t)\rangle = \sum_{l=1}^{N} c_{j,l}(t)|k\rangle$.

The recipe contains two key steps: (i) propagation (step 3) and (ii) determination of the time of the next jump (step 4). The waiting time, i.e., the time between two consecutive jumps, cannot be obtained without actual propagation of the trajectory (except in a few cases [24,36]). This time must be obtained along with the numerical integration by using the non-Hermitian Hamiltonian $\tilde{H}(t)$. One has to propagate a trajectory, monitor the decaying squared norm of the wave vector and determine the instant of time when the squared norm equals the randomly chosen value η. In most of the existing studies, this was realized with a step-by-step Euler method. This approach, although having a physical interpretation [36], is not suitable for our purpose because it corresponds to the expansion of Eq. (1) to the first order in a time step δt; consequently, a reasonable accuracy of the sampling can be achieved with extremely small values of δt only [42].

Several improvements based on higher-order (with respect to δt) unraveling schemes [45,46] have been put forward. The accuracy of the sampling—for the same number of realizations M_r and time step δt—can be improved substantially by increasing the order of the integration scheme [45]. In QuTiP, an open-source toolbox in Python to simulate dynamics of open quantum systems [33], Adams method (up to 12th order) and backward differentiation formula (up to fifth order) with adaptive time step are implemented. In this respect, this is presently the most advanced implementation, to the best of our knowledge. In addition, QuTiP supports time-dependent Hamiltonians and allows for multi-processor parallelization. The original publication [33] addressed scalability and performance of the QuTiP package and demonstrated that a stationary model with $N = 8000$ states can be propagated. However, the results remained restricted to averaging over a few quantum trajectories and relatively short propagation time t_p. Also, the issues of accuracy and convergence to an asymptotic state with the number of sampled trajectories were not discussed.

In contrast, aside of reaching large N, we are concerned about the following two issues. First, there is the accuracy of propagation. As t_p has to be extremely large in order to be able to sample a state close to the attractor state ϱ^{att} (note that up to now the method of quantum trajectories was used mainly to analyze short-time relaxation and transient regimes in terms of some observables; e.g., see in Refs. [23]), the accumulating error due to the discrete approximation of the continuous evolution with the effective Hamiltonian $\tilde{H}$ can emerge sizable. These errors may cause serious problems, for example, when dealing with the delicate issue of MBL phenomena. Second, in the limit of weak dissipation, when the coupling rates γ_k are small, jumps occur rarely. For most of the time the evolution of the trajectory is deterministic and propagation using a small δt will not be efficient. Increasing the time step implies a decrease of the accuracy of determination of the time of the jump. This constitutes yet another factor which can blur the quality of the sampling scheme. On the other side, we want to maximize the speed (in terms of computational time) of the propagation. If these two problems are successfully overcome, the only remaining problem left is to obtain a sufficiently large number of realizations. Here, we handle both issues with an approach presenting an alternative to the schemes which rely on increasing the order of integration.

A quantum trajectory is an example of a so-called "event-driven process" used in control theory [47] (where they are also known as "Lebesgue sampling processes") and likewise also in computational neuroscience [48]. The question how to integrate such processes *numerically exact* has been discussed in those research areas already since the late 1990s. A possible option consists in the combination of an exponential propagation together with time-stepping techniques. We next mainly follow the idea put forward with Ref. [48].

To start, let us first consider a time-independent Hamiltonian $H(t) \equiv H$. The propagation over any time interval δt with the corresponding effective Hamiltonian $\tilde{H}$ can be done by the propagating operator (propagator) $P_{\delta t} = e^{-i\tilde{H}\delta t}$. Exponentiation of $\tilde{H}$ can be performed numerically with a controllable accuracy [49]. To determine the time of the

next jump, we use a time stepping technique [48]. We choose the convenient and efficient bisection method [50], cf. Sec. V for more details. The accuracy of the bisection method is controlled by the maximal order of bisections S which we call "maximal depth." The time of the jump is thus resolved with a precision $2^{-S}\delta t$. A practical realization of this method demands a set of S propagators, that is, $P_{\delta t_s} = e^{-i\tilde{H}\delta t_s}$, $\delta t_s = 2^{-s}\delta t_0$, $s = 0,...,S$, that are complex $N \times N$ matrices. These propagators have to be pre-calculated and then stored. Generalization of this approach to the case of quenchlike temporal modulations is straightforward. In the bi-Hamiltonian case, Eq. (2), we have to double the number of the stored propagators and then switch between the two sets every half of the period T.

Our key objective here is to estimate the maximal system size N for Eqs. (1) and (2), whose asymptotic density matrix can be resolved with quantum trajectories implemented on a computational cluster and validate the accuracy of the sampling algorithm.

III. STATISTICAL ERROR(S) OF SAMPLING

We next discuss the problem of statistical errors. We assume that the integration of quantum trajectories is performed in a numerically exact way, i.e., when the list of consequent norm thresholds, $\eta = \{\eta_1,\eta_2,...,\eta_n\}$, and the initial state, $\varrho^{\text{init}} = |\psi^{\text{init}}\rangle\langle\psi^{\text{init}}|$, are given, the corresponding trajectory can be calculated with any prescribed accuracy ϵ. More precisely, it can be calculated such that $\forall t < t_p$ we have $\||\psi(t)\rangle - |\psi^{\text{exact}}(t)\rangle\| \leqslant \epsilon$, where $\|.\|$ is some suitable norm and $t_p[\eta,|\psi^{\text{init}}\rangle]$ is the propagation time.

Consider the sampling of a variable $X(t)$ over an ensemble of realizations $\{X_j(t)\}$, $j = 1,...,M_r$, with the aim to estimate its mean $\tilde{X}(t)$. Examples would be the expectation value of an operator [36–39] or an element of the density matrix (as in our case). In addition to the mean (average) of the variable, $\tilde{X}(t;M_r) = \frac{1}{M_r}\sum_{j=1}^{M_r} X_j(t)$, we can also calculate its variance [24,39],

$$\text{var}[X(t);M_r] = \frac{1}{M_r}\sum_{j=1}^{M_r}(X_j(t) - \tilde{X}(t;M_r))^2, \tag{5}$$

which here for systems possessing a finite Hilbert space dimension N is assumed to converge to a generally time-dependent value $\text{var}[X(t)]$ in the limit $M_r \to \infty$. Different trajectories are statistically independent. Therefore, the central limit theorem applies and, for large M_r, the probability density function (pdf) of the mean $\tilde{X}(t;M_r)$ can be approximated by a Gaussian pdf centered at $\tilde{X}(t)$ with the standard deviation $\sigma(t;M_r) = \sqrt{\text{var}(X;M_r)/M_r} \overset{M_r\gg 1}{\propto} M_r^{-\frac{1}{2}}$.

In the framework of local and global quantities [37], elements of the density matrix correspond to the former. That means that in order to resolve their values we need $M_r \gg N$ realizations. In addition, they are small for large N, $\varrho_{kl} \sim \mathcal{O}(N^{-1})$, and the standard criterion of a trustful sampling, $\sigma(M_r)/\varrho_{kl} \ll 1$, implies that $M_r \gg N^2$. Such a massive sampling is unfeasible if $N \gtrsim 10^3$, even on a supercomputer. However, this constitutes a sufficient condition which greatly overestimates (hopefully) the number of realizations needed for a reasonable resolution of the density matrix, as we scrutinize for our test case below. This presents yet another aspect of the sampling with quantum trajectories we aim to gain more specific insight.

Another issue we like to mention is the time evolution of the variance $\text{var}[\varrho_{kl}(t)]$. Evidently, it cannot grow to infinity simply because the absolute values of the coefficients $c_s(t)$ do not exceed one. Therefore, there is an upper limit $\text{var}[\varrho_{kl}(t)] \simeq 1$. On the other hand, for completely random and uniformly distributed values of $c_s(t)$ we find $\text{var}[\varrho_{kl}(t)] \propto N^{-1}$. By using a scalable model we show that (i) the variances saturate in course of propagation to time-periodic values, $\text{var}[\varrho_{kl}(t+T)] = \text{var}[\varrho_{kl}(t)]$, which in addition (ii) allow for an accurate estimation of the density matrix elements with less than N^2 realizations.

IV. A MODEL

As a test bed for the algorithm we use an open physical system made up of $N-1$ indistinguishable interacting bosons which hop between two sites, with on-site energies periodically varied in time. The system Hamiltonian reads

$$H(t) = -J(b_1^\dagger b_2 + b_2^\dagger b_1) + \frac{U}{2(N-1)}\sum_{g=1,2} n_g(n_g-1) + \varepsilon(t)(n_2 - n_1). \tag{6}$$

Here, J denotes the tunneling amplitude, U is the interaction strength, and $\varepsilon(t)$ presents a periodically varying modulation of the local potential in time. In particular, we choose $\varepsilon(t) = \varepsilon(t+T) = \mu_0 + \mu_1 Q(t)$, where μ_0 and μ_1 denote a static and a dynamically varying, respectively, energy offset between the two sites. $Q(t)$ itself is a periodically varying, unbiased two-valued quench-function within one full period T; more specifically, $Q(\tau) = \frac{1}{2}$ within $0 < \tau \leqslant T/2$ and $Q(\tau) = -\frac{1}{2}$ for the second half period $T/2 < \tau \leqslant T$. The boson operators b_g and $b_g^\dagger$ are the annihilation and creation operators on site $g \in \{1,2\}$, while $n_g = b_g^\dagger b_g$ is the particle number operator. The system Hilbert space has dimension N and can be spanned with the N Fock basis vectors, labeled by the number of boson on the first site n, $\{|n+1\rangle\}$, $n = 0,...,N-1$. Thus, the model size is controlled by the total number of bosons. The Hamiltonian Eq. (6) has been used for theoretical studies before in Refs. [51–55] and, as well, has been implemented in recent experiments [56,57].

For the single jump operator we use [58]

$$V = (b_1^\dagger + b_2^\dagger)(b_1 - b_2), \tag{7}$$

which attempts to "synchronize" the dynamics on the sites by constantly recycling anti-symmetric out-phase modes into symmetric in-phase ones. The dissipative coupling constant $\gamma = \gamma_0/(N-1)$ is taken to be time-independent. Since the jump operator is non-Hermitian, the propagators $\mathcal{P}_t$ are not unital and the attractor does not assume the maximally mixed state, $\varrho^{\text{att}} \neq \mathbb{1}/N$.

The Hamiltonian Eq. (6) is nonintegrable when $U \neq 0$; therefore, an analytical solution of the corresponding Lindblad equation is not available. However, in the limit $N \to \infty$ the dynamics can be approximated by mean-field equations for the expectation values of the three pseudospin operators

$\mathcal{S}_x = \frac{1}{2(N-1)}(b_1^\dagger b_2 + b_2^\dagger b_1)$, $\mathcal{S}_y = -\frac{i}{2(N-1)}(b_1^\dagger b_2 - b_2^\dagger b_1)$, $\mathcal{S}_z = \frac{1}{2(N-1)}(n_1 - n_2)$. For a large number of atoms, the commutator $[\mathcal{S}_x,\mathcal{S}_y] = [i\mathcal{S}_z/(N-1)] \overset{N\to\infty}{=} 0$ and similarly for other cyclic permutations. Replacing operators with their expectation values, $\langle \mathcal{S}_k \rangle = \mathrm{tr}[\varrho \mathcal{S}_k]$, and denoting $\langle \mathcal{S}_k \rangle$ by S_k, we find the semiclassical equations of motion [59],

$$\begin{aligned} \frac{dS_x}{dt} &= 2\varepsilon(t)S_y - 2US_zS_y + 8\gamma_0\left(S_y^2 + S_z^2\right), \\ \frac{dS_y}{dt} &= -2\varepsilon(t)S_x + 2US_xS_z + 2JS_z - 8\gamma_0 S_xS_y, \\ \frac{dS_z}{dt} &= -2JS_y - 8\gamma_0 S_xS_z. \end{aligned} \tag{8}$$

As $S^2 = S_x^2 + S_y^2 + S_z^2 = 1/4$ is a constant of motion, we can reduce the mean-field evolution to the surface of a Bloch sphere, $(S_x,S_y,S_z) = \frac{1}{2}[\cos(\varphi)\sin(\vartheta), \sin(\varphi)\sin(\vartheta), \cos(\vartheta)]$, yielding the equations of motion,

$$\begin{aligned} \dot{\varphi} &= 2J\frac{\cos(\vartheta)}{\sin(\vartheta)}\cos(\varphi) - 2\varepsilon(t) + U\cos(\vartheta) - 4\gamma_0\frac{\sin(\varphi)}{\sin(\vartheta)}, \\ \dot{\vartheta} &= 2J\sin(\varphi) + 4\gamma_0\cos(\varphi)\cos(\vartheta). \end{aligned} \tag{9}$$

The density matrix ϱ of the system with $(N-1)$ bosons can be visualized on the same Bloch sphere by plotting the Husimi distribution $p(\vartheta,\varphi)$, obtained by projecting ϱ on the set of the generalized SU(2) coherent states, $|\theta,\varphi\rangle = \sum_{j=0}^{N-1}\sqrt{\binom{N-1}{j}}[\cos(\theta/2)]^j[e^{i\phi}\sin(\theta/2)]^{N-1-j}|j\rangle$ [60,61]. The visual comparison of the Husimi distribution with the mean-field solution, Eq. (9), will serve as a test of the meaningfulness of the sampled density matrix $\varrho(t_p; M_r)$.

V. IMPLEMENTATION ON A CLUSTER AND PERFORMANCE

Next we describe a high-performance implementation of the algorithm on a supercomputer and analyze the scalability of its implementation by using the model system Eqs. (6) and (7). Numerical experiments were performed on the "Lobachevsky" supercomputer [62] at the Lobachevsky State University of Nizhny Novgorod. We employed up to 32 computing nodes, with the following configuration per node: 2× Intel Xeon E5-2660 CPU (8 cores, 2.2 GHz), 64 GB RAM, OS CentOS 6.4. We use Intel Math Kernel Library (MKL), Intel C/C++ Compiler, and Intel MPI from Intel Parallel Studio XE [63].

Using Eq. (3), we start with two effective non-Hermitian Hamiltonians, $\tilde{H}_1$ and $\tilde{H}_2$, describing the quenchlike modulations, Eq. (2), as represented by a pair of complex double-precision $N \times N$ matrices. An initial pure state $|\psi^{\mathrm{init}}\rangle$ is represented by a complex-valued double-precision vector. The propagation operator yields a wave function for a single sample. We follow the straightforward approach to parallelization with an independent random sampling. Namely, the computational load is distributed among supercomputer nodes by the standard Message Passing Interface (MPI). On each node we employ the OpenMP threads to parallelize sampling. Computationally intensive operations are implemented by calling BLAS functions from Intel MKL in sequential mode.

The code consists of three main steps. First, the program initializes MPI, allocates memory, and reads parameters and the matrices of the precalculated exponential propagators from configuration files. The propagators are calculated independently on each cluster node. On the second step all OpenMP threads in all MPI processes independently propagate several quantum trajectories starting from the initial state $|\psi^{\mathrm{init}}\rangle$ [64].

The propagation is realized by using the step-decimation technique [65]. This pseudocode is presented in Algorithm 1. The maximal depth S, the time steps $\delta t_s = 2^{-s}dt$, and the exponential propagators $P_{\delta t_s}$, $s = 0,...,S$ are preloaded. The program is initiated with $s = 0$, but later on s is taken from the previous propagation loop step. This step is fully parallel; it contains a matrix-vector multiplication that is the most computationally intensive part of the algorithm. This operation is performed with the $zgemv$ MKL subroutine. During the third step all samples on each node are accumulated into the density matrix. Next, these matrices are collected in the rank 0 MPI process. Finally, one evaluates the resulting density matrix. This matrix is written to the output file, the dynamic memory is deallocated and the MPI is finalized.

The efficient utilization of a supercomputer requires a reasonable scaling on the distributed memory. In this regard, quantum trajectories possess an ideal parallelization potential. The method realizes the general Monte Carlo paradigm with independent simulations and without substantial load imbalance. The transfer of the resulting data is the only data interchange between nodes. We ran numerical simulations utilizing up to 32 nodes of the supercomputer and found that the implementation scales almost linearly with the number of nodes. Next, we consider the performance and the scaling efficiency of the implementation on 16 CPU cores with shared memory. To start, the number of MPI processes and OpenMP threads have to be chosen. We tried several different configurations; namely, 1 process × 16 threads, 2 processes × 8 threads, 4 processes × 4 threads, 8 processes × 2 threads, and 16 processes × 1 thread. We did not find a substantial difference in performance and chose the option 1 MPI process with 16 OpenMP threads mode for illustration. It is known that setting a relevant affinity mask to pin threads to CPU cores usually affects performance and scalability. In this regard, we used the following settings: `KMP_AFFINITY= granulatiny= fine, scatter`. For all performance measurements in this section we considered the model setup, Eqs. (6) and (7), with 63 bosons (i.e., with dimension $N = 2^6 = 64$) and 640 trajectories. The results of our computational experiments are summarized in Table I. Upon inspection this shows that our implementation allows 87% scaling efficiency on 16 CPU cores with shared memory.

Then, we ran the Intel VTune Amplifier XE profiler to find main time-consuming parts of our implementation. As a result we found that the high-performance implementation of the dense matrix-vector multiplication with $zgemv$ takes more than 99% of the total computation time. This in turn means that there is no potential for further optimization of the code.

Finally, we estimate the computation time to propagate a single trajectory on a single-core as a function of system size

TABLE I. Scaling efficiency on shared memory.

Number of threads	Time of computations, in seconds	Efficiency, percent
1	2170	100
2	1114	97
4	557	97
8	292	93
16	156	87

N; see Table II. For the model specified by Eqs. (6) and (7) this time scales as N^3; this is due to the multiplication of the quadratic scaling of a dense matrix-vector multiplication and a linear scaling of the jump frequency. The latter scaling is, however, model specific and may differ for other models. Thus, the overall computation time may vary substantially with the type of Hamiltonian or/and dissipators under study. On top, the values we present in Table I depend on the values of the coupling constant γ_0 and the period of modulations T. This is so because these parameters control the rate of the jumps. Therefore, these obtained estimates should not be taken as invariant quantifiers.

VI. APPLICATIONS

We now report the results of our simulations obtained for the model given by Eqs. (6) and (7). We start with the performance of the algorithm, Table I. The idea of the algorithm mimics a float: The algorithm constantly attempts to "float to the surface," i.e., to increase the time step of integration toward its maximal value δt_0, while every next jump pulls it downwards to δt_S; see Fig. 1. The average time between two consequent jumps is the mean of the local maxima in the depicted sawlike time sequence of δt. There is no problem in overestimating δt_0, simply because the time step will rarely reach its maximum. The shortest time step, δt_S, or, equivalently, the depth S, is tuned to the values needed to reach the desired accuracy.

Next we turn to the averages $\bar{\varrho}^{\rm att}_{kl}(t)$ over realizations and the corresponding statistical variances $\mathrm{var}[\varrho^{\rm att}_{kl}(t)]$ of the matrix elements. Both quantifiers converge to "limit cycles" if the propagation time $t_p = nT + \tau$, $n \in \mathbb{Z}^+$, $\tau \in [0,T)$, is much larger than all relaxation times. This means that for $n \gg 1$

TABLE II. Single-core computation time to propagate a trajectory over one period T as a function of N. The parameters are $J = 1$, $\mu_0 = 1.5$, $\mu_1 = 1$, $U = 3$, $\gamma_0 = 0.1$, and $S = 20$.

Number of states, N	Time of computations, in seconds
64	0.37
128	2.3
256	16
512	153
1024	1153
2048	8642
4096[a]	64 785

[a]Extrapolation

Algorithm 1: Propagation of a quantum trajectory with exponential operators and bisection method

set $\delta t = \delta t_0$ & $s = 0$
While $\||\psi(t)\rangle\|^2 > \eta$ **do**
  calculate $|\tilde{\psi}(t)\rangle = P_{\delta t}|\psi(t)\rangle$
  if $\||\tilde{\psi}(t)\rangle\|^2 < \eta$ & $s < S$ **then**
    $s = s + 1$; $\delta t = \delta t/2$
  else
    $|\psi(t)\rangle = |\tilde{\psi}(t)\rangle$
    $t = t + \delta t$
    While $s > 0$ & $\delta t = n \cdot \delta t_{s-1}$, $n \in \mathbb{Z}^+$ **do**
      $s = s - 1$; $\delta t = \delta t_s$
  end while
  end if
end while

the density matrix converges to a time-periodic quantum attractor, i.e., $\bar{\varrho}^{\rm att}(t+T) = \bar{\varrho}^{\rm att}(t)$ [see Fig. 2(a)] and the variances also become time-periodic functions, $\mathrm{var}[\varrho^{\rm att}_{kl}(t+T)] = \mathrm{var}[\varrho^{\rm att}_{kl}(t)]$ [see Fig. 2(b)]. The crumpled causticlike shapes of the limit cycles is a result of the projection of a limit-cycle living in a high-dimensional space on a plane. These limit cycles are not topological products of N^2 two-dimensional limit cycles; elements of the density matrix do not evolve independently and their means and variances are correlated.

For relatively small system sizes, $N \simeq 100$, we can obtain a numerically exact asymptotic solution, calculated as the kernel of the Floquet map minus identity, $(\mathcal{P}_T - \mathbb{1})\varrho^{ex}(0) = 0$. It allows us to quantify convergence of the sampled density matrix—with the increase of the number of sampled trajectories, M_r—to the asymptotic state. The error is defined as the spectral norm [66] of the difference matrix, $\epsilon = \|\bar{\varrho}^{\rm att}(mT) - \varrho^*(\tau = 0)\|$. We find that, for the chosen set of parameters, the sampled solution converges to an attractor

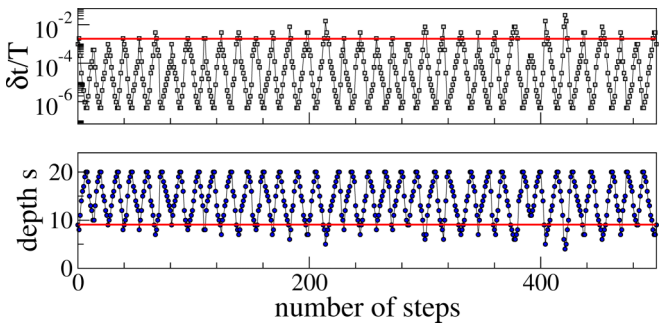

FIG. 1. Floatlike performance of Algorithm II during the propagation of a quantum trajectory. Every local maximum in the dependence δt vs. number of steps (minimum in the depth s dependence) indicates an occurrence of a jump after which the algorithm performs a chain of bisections to reach the maximal depth $S = 20$. After every step during which no jump occurred, the algorithm doubles the step size. The average time between two consecutive jumps (red line) is the average height of the local maximum minus 1. The two sequences were monitored during the sampling of the asymptotic state.

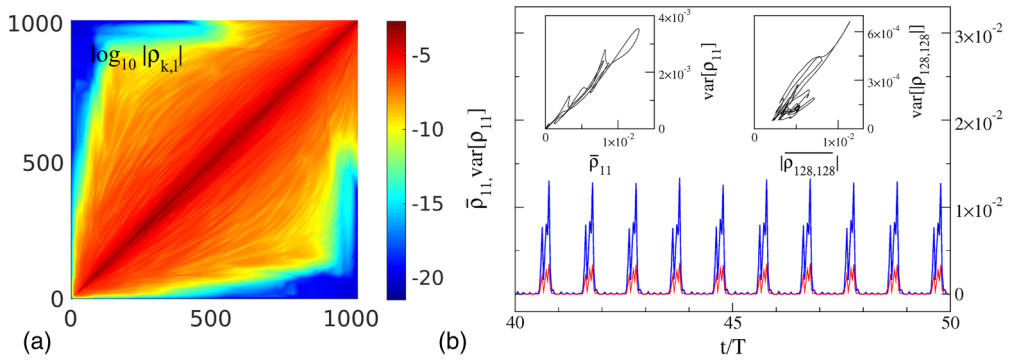

FIG. 2. (a) Structure of the sampled stroboscopic density matrix $\varrho^{\rm att}(0)$ ($N = 1024$) and (b) time evolution of the mean $\bar{\varrho}_{11}(t)$ (thick blue line) and variance $\mathrm{var}[\varrho_{11}(t)]$ (thin red line) for $t \in [40T, 50T]$. The system size is $N = 256$ and the sampling was performed over 10^5 independent trajectories initiated at the state $|\psi^{\rm init}\rangle = |1\rangle$ and then propagated to the time $t_p = 50T$. The inset depicts the limit-cycle evolution of the means and variances for two diagonal elements, $\varrho_{1,1}$ and $\varrho_{128,128}$, during one period of modulations, $t \in [1000T, 1001T]$. Curves for later periods are indistinguishable from the presented ones. The parameters are the same as in Fig. 1.

already after $t_p \simeq 50T$, such that for $t > t_p$ the observed error remains essentially time-independent. The resulting plot demonstrates that the sampling error scales as $1/\sqrt{M_r}$ (as expected for an independent Monte Carlo sampling) with no signatures of saturation; see Fig. 3.

In the asymptotic regime, the sampling can be performed stroboscopically, i.e., after every period T. In our simulations we used $t_p = 1000T$ as the transient time and then performed the stroboscopic sampling of $\varrho^{\rm att}(\tau = 0)$. The attractor density matrix at any other instant of time $\tau \in [0, T]$ can be sampled by shifting the starting time of the sampling, $t_p \to t_p + \tau$, or also by performing an extra-sampling at all needed intermediate points.

With 4000 samples per trajectory (that amounts to an additional propagation over the time $4000T$) it became possible to collect $M_r = 10^5$ samples for the model system of the dimension $N = 1024$ (i.e., $N - 1 = 1023$ indistinguishable bosons) by running the program on 32 cores during three days. The Husimi distribution of the sampled density matrix is depicted in Fig. 4. There is an intriguing similarity between the distribution of the quantum attractor and the phase-space structure of the classical attractor (its stroboscopic section, to be more precise) produced by the mean-field equations. This allows us to conjecture that the attractor density matrix is resolved with a good accuracy. The 128 cores allowed us to sample the same number of realizations for the model with dimension $N = 2048$ during approximately one week [67].

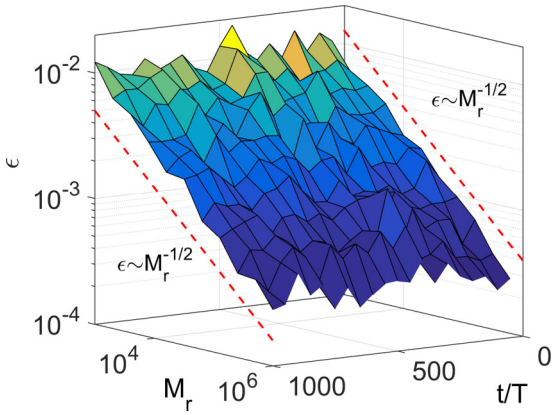

FIG. 3. Spectral norm of the difference between the density matrix stroboscopically sampled with quantum trajectory algorithm and numerically exact asymptotic solution, $\epsilon = \|\bar{\varrho}^{\rm att}(mT) - \varrho^{ex}(\tau = 0)\|$, for the two-mode model, Eqs. (6) and (7). Here $N = 100$, $J = 1$, $\mu_0 = 1.5$, $\mu_1 = 1$, $U = 3$, $\gamma_0 = 0.1$.

VII. CONCLUSIONS

The objective of this study was to estimate the numerical horizon of a high-accuracy sampling of nonequilibrium dissipative states of periodically driven quantum systems by using a high-precision realization of the quantum trajectory method.

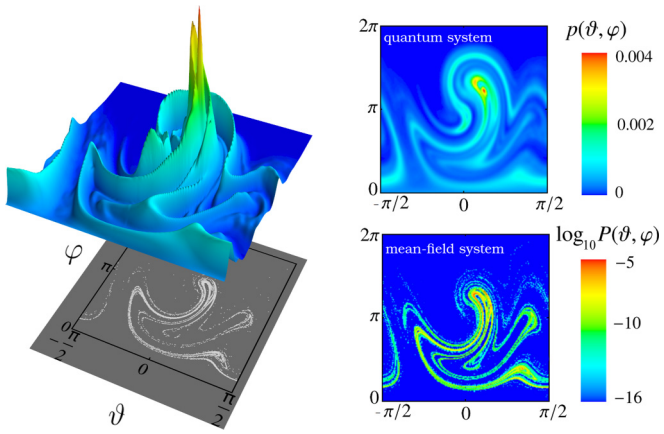

FIG. 4. Attractors of the two-mode model, Eqs. (6) and (7), with $N - 1 = 1023$ bosons. Left panel: Husimi distribution $p(\vartheta,\varphi)$ of the stroboscopic density matrix $\varrho^{\rm att}(0)$ (top) and Poincaré plot of the attractor of the corresponding mean-field system, Eq. (8) (bottom). The density matrix was sampled with 10^5 stroboscopic realizations. Right panel: Plane version of $p(\vartheta,\varphi)$ (top) compared to the probability density function (pdf) $P(\vartheta,\varphi)$ of the classical mean-field attractor (bottom). The pdf was estimated by sampling the histogram on a 200×200 bin grid with 10^8 stroboscopic points. Note that, because of a high localization of the density near point $(0, 3\pi/2)$, the logarithmic scale is used. The parameters are $J = 1$, $\mu_0 = 1.5$, $\mu_1 = 1$, $U = 3$, $\gamma_0 = 0.1$.

We demonstrated that, by implementing the algorithm on a cluster with $\leqslant 128$ cores, it is possible to resolve time-periodic asymptotic density operator of driven open quantum systems of several thousand of states on a time scale of a few days. The benefit of gaining access to the whole density matrix is the possibility to extract more detailed information about the nonequilibrium regimes such as the purity and many-body entanglement [59].

We would like to surmise on possible optimization of the sampling procedure. An immediate idea is to use an optimal initial state $|\psi^{\text{init}}\rangle$ to reduce the transient time t_p. When it is about resolving the asymptotic density operator as a function of the value of a parameter changed within some range, the last moment wave vectors for the current parameter value can be used as the initial states to sample operator for the next parameter value. Next, the performance of the algorithm can be substantially increased by grouping trajectories into matrices and substituting a set of matrix-vector multiplications with a single matrix-matrix multiplication. Our tests have shown that even in the presence of intrinsic asynchrony between different trajectories, this modification leads to a more than tenfold acceleration of the sampling process [68].

Research areas where many-body "quantum attractors" are of potential interest have been already mentioned in the introduction. We like to recall them.

First, this is many-body localization [19] where the action of temporal modulations [20,21] and dissipation [22,23] so far have been considered separately. A combined action of both factors on the ergodic-MBL transition presents an intriguing challenge. The survival of Floquet topological insulators [15] in the presence of dissipation or creation of new types of insulating Floquet states with synthetic dissipators are objectives of interest for practical applications.

Second, a large-scale accurate sampling of nonequilibrium many-body states can serve a useful tool to explore non-Markovian quantum systems [69]. There is a branch of related studies where non-Markovian effects are realized by using different modification of quantum trajectory method, e.g., generalizations to the case of time-dependent temporarily negative dissipative rates $\gamma_k(t)$, Eq. (1) [70]. Non-Markovian evolution can also be obtained for a system $\mathcal{A}$, a part of a bipartite system in which the second part $\mathcal{B}$ is subjected to continuous measurements [71]. The evolution of the total system $\mathcal{A}+\mathcal{B}$ is Markovian and therefore can be performed by using the standard quantum trajectory technique; the density matrix of system $\mathcal{A}$ will be obtained by tracing out $\mathcal{B}$. Asymptotic Floquet states of periodically driven non-Markovian systems [72] are intriguing objects per se.

Third, a numerically exact realization of quantum trajectory method can be used to analyze—in a very accurate way—the thermodynamics of quantum jump trajectories [73] in complex periodically modulated open quantum systems and search for nonequilibrium analogs of dissipative phase transitions [74].

Finally, we would like to mention an alternative to quantum trajectory method that is the unraveling of the Lindblad Eq. (1) into a set of realizations generated by a stochastic Schrödinger equation (SSE) [24]. There are real-life physics behind these equations; on the microscopic level they can be deduced from the dynamics of systems subjected to continuous quantum measurements. There is a selection of numerical methods to integrate SSEs that are adapted from the toolbox developed for classical stochastic equations [75], such as the Heun scheme and different stochastic Runge-Kutta schemes [24]. Implementations of these methods on computational clusters may open a complimentary path to many-body quantum attractors.

ACKNOWLEDGMENTS

The authors acknowledge support of the Russian Science Foundation Grant No. 15-12-20029. The authors also thank I. Vakulchik for the help with preparing the figures.

[1] B. Kraus, H. P. Büchler, S. Diehl, A. Kantian, A. Micheli, and P. Zoller, Phys. Rev. A **78**, 042307 (2008).
[2] D. Witthaut, F. Trimborn, and S. Wimberger, Phys. Rev. Lett. **101**, 200402 (2008).
[3] G. Kordas, S. Wimberger, and D. Witthaut, Phys. Rev. A **87**, 043618 (2013).
[4] J. T. Barreiro *et al.*, Nat. Phys. **6**, 943 (2010).
[5] D. Kienzler *et al.*, Science **347**, 53 (2015).
[6] F. Pastawski, L. Clemente, and J. I. Cirac, Phys. Rev. A **83**, 012304 (2011).
[7] M. J. Kastoryano, M. M. Wolf, and J. Eisert, Phys. Rev. Lett. **110**, 110501 (2013).
[8] J. H. Shirley, Phys. Rev. **138**, B979 (1965).
[9] H. Sambe, Phys. Rev. A **7**2203 (1973).
[10] M. Grifoni and P. Hänggi, Phys. Rep. **304**, 229 (1998).
[11] S. Kohler, J. Lehmann, and P. Hänggi, Phys. Rep. **406**, 379 (2005).
[12] A. Eckardt and E. Anisimovas, New J. Phys. **17**, 093039 (2015).
[13] M. Bukov, L. D'Alessio, and A. Polkovnikov, Adv. Phys. **64**, 139 (2015).
[14] J. Gong, L. Morales-Molina, and P. Hänggi, Phys. Rev. Lett. **103**, 133002 (2009).
[15] N. H. Lindner, G. Refael, and V. Galitski, Nat. Phys. **7**, 490 (2011).
[16] D. E. Liu, A. Levchenko, and H. U. Baranger, Phys. Rev. Lett. **111**, 047002 (2013); A. Kundu and B. Seradjeh, *ibid.* **111**, 136402 (2013).
[17] N. Goldman and J. Dalibard, Phys. Rev. X **4**, 031027 (2014).
[18] A. Eckardt, Rev. Mod. Phys. **89**, 011004 (2017).
[19] D. M. Basko, I. L. Aleiner, and B. L. Altshuler, Ann. Phys. **321**, 1126 (2006).
[20] P. Ponte, Z. Papić, F. Huveneers, and D. A. Abanin, Phys. Rev. Lett. **114**, 140401 (2015).
[21] A. Lazarides, A. Das, and R. Moessner, Phys. Rev. Lett. **115**, 030402 (2015).
[22] M. H. Fischer, M. Maksymenko, and E. Altman, Phys. Rev. Lett. **116**, 160401 (2016).
[23] E. Levi, M. Heyl, I. Lesanovsky, and J. P. Garrahan, Phys. Rev. Lett. **116**, 237203 (2016).

[24] H.-P. Breuer and F. Petruccione, *The Theory of Open Quantum Systems* (Oxford University Press, Oxford, 2002).

[25] H. J. Carmichael, *An Open Systems Approach to Quantum Optics* (Springer, Berlin, 1993).

[26] G. Lindblad, Commun. Math. Phys. **48**, 119 (1976).

[27] R. Alicki and K. Lendi, *Quantum Dynamical Semigroups and Applications*, Lecture Notes in Physics (Springer, Berlin, 1998), Vol. 286.

[28] A. Lazarides, A. Das, and R. Moessner, Phys. Rev. E **90**, 012110 (2014).

[29] L. D'Alessio and M. Rigol, Physical Review X **4**, 041048 (2014).

[30] V. A. Yakubovich and V. M. Starzhinski, *Linear Differential Equations with Periodic Coefficients* (John Wiley & Sons, New York, 1975).

[31] P. D. Nation, J. R. Johansson, M. P. Blencowe, and A. J. Rimberg, Phys. Rev. E **91**, 013307 (2015).

[32] Even if the Hamiltonians H_1, H_2 and the Lindblad operators $\mathcal{L}_1$, $\mathcal{L}_2$ are sparse; thus, the Floquet map $\mathcal{P}(T) = e^{\mathcal{L}_2(T-\tau)}e^{\mathcal{L}_1\tau}$ yields a dense matrix. Therefore, the numerical evaluation cannot benefit from sparse matrix methods.

[33] R. Johansson, P. D. Nation, and F. Nori, Comput. Phys. Commun. **183**, 1760 (2012).

[34] W. Huisinga, L. Pesce, R. Kosloff, and P. Saalfrank, J. Chem. Phys. **110**, 5538 (1999).

[35] There is a sophisticated way to propagate Eq. (1) by using the time evolving block decimation (TEBD) technique [40,41]. The corresponding numerical effort scales as $\log N$. However, this algorithm can only be used for systems of lattice topology, i.e., systems that can be partitioned into $\sim \log(N)$ "pieces" coupled by next-neighbor interactions, both unitary and dissipative. In this case it yields the correct answer when the asymptotic state is characterized by a short-range entanglement.

[36] R. Dum, A. S. Parkins, P. Zoller, and C. W. Gardiner, Phys. Rev. A **46**, 4382 (1992).

[37] K. Mølmer, Y. Castin, and J. Dalibard, J. Opt. Soc. Am. B **10**, 524 (1993).

[38] M. B. Plenio and P. L. Knight, Rev. Mod. Phys. **70**, 101 (1998).

[39] A. J. Daley, Adv. Phys. **63**, 77 (2014).

[40] F. Verstraete, J. J. Garcia-Ripoll, and J. I. Cirac, Phys. Rev. Lett. **93**, 207204 (2004).

[41] M. Zwolak and G. Vidal, Phys. Rev. Lett. **93**, 207205 (2004).

[42] A generalization of the TEBD technique to non-Hermitian operators was used for the propagation step in Refs. [43,44]. Similar to its Hermitian predecessor, that method can only be implemented for lattice systems. Also, it guarantees correct asymptotic results only when there no distant entanglement build-ups in the course of the system evolution.

[43] A. J. Daley, J. M. Taylor, S. Diehl, M. Baranov, and P. Zoller, Phys. Rev. Lett. **102**, 040402 (2009).

[44] L. Bonnes and A. M. Läuchli, arXiv:1411.4831 (2014).

[45] J. Steinbach, B. M. Garraway, and P. L. Knight, Phys. Rev. A **51**, 3302 (1995).

[46] H.-P. Breuer, U. Dorner, and F. Petruccione, Comput. Phys. Commun. **132**, 30 (2000).

[47] K. Aström and B. Bernhardsson, in *Proceedings of the IFAC World Conference* (Lund University, 1999), pp. 301–306.

[48] S. Rotter and M. Diesmann, Biol. Cybern. **81**, 381 (1999).

[49] To exponentiate the effective Hamiltonian, one can use any method with controllable accuracy, e.g., Padé approximation and various splitting algorithms; see C. Moler and Ch. Van Loan, SIAM Rev. **45**, 3 (2003). Since this operation is performed only once, at the beginning, its computational cost is not relevant. We used the standard MATLAB routine, *expm*, which implements the scaling and squaring method (there are also alternatives, *expmdemo*1, *expmdemo*2, and *expmdemo*3, which use Padé approximation, Taylor series approximation, and eigenvalues and eigenvectors, respectively).

[50] D. E. Knuth, *The Art of Computer Programming* (Pearson Edition, US, 1998), Vol. 3.

[51] A. Vardi and J. R. Anglin, Phys. Rev. Lett. **86**, 568 (2001).

[52] F. Trimborn, D. Witthaut, and S. Wimberger, J. Phys. B: At. Mol. Opt. Phys. **41**, 171001 (2008).

[53] D. Witthaut, F. Trimborn, H. Hennig, G. Kordas, T. Geisel, and S. Wimberger, Phys. Rev. A **83**, 063608 (2011).

[54] D. Poletti, J.-S. Bernier, A. Georges, and C. Kollath, Phys. Rev. Lett. **109**, 045302 (2012).

[55] G. Kordas, D. Witthaut, P. Buonsante, A. Vezzani, R. Burioni, A. I. Karanikas, and S. Wimberger, Eur. Phys. J.: Spec. Top. **224**, 2127 (2015).

[56] C. Gross, T. Zibold, E. Nicklas, J. Esteve, and M. K. Oberthaler, Nature **464**, 1165 (2010).

[57] J. Tomkovič, W. Muessel, H. Strobel, S. Löck, P. Schlagheck, R. Ketzmerick, and M. K. Oberthaler, Phys. Rev. A **95**, 011602(R) (2017).

[58] S. Diehl, A. Micheli, A. Kantian, B. Kraus, H. P. Büchler, and P. Zoller, Nat. Phys. **4**, 878 (2008).

[59] M. Hartmann, D. Poletti, M. Ivanchenko, S. Denisov, and P. Hänggi, New J. Phys. **19**, 083011 (2017).

[60] F. T. Arecchi, E. Courtens, R. Gilmore, and H. Thomas, Phys. Rev. A **6**, 2211 (1972).

[61] A. Perelomov, *Generalized Coherent States and Their Applications* (Springer, Berlin 1986).

[62] http://www.top500.org/system/178472.

[63] Intel® Parallel Studio XE 2015, https://software.intel.com/en-us/intel-parallel-studio-xe.

[64] The components of the initial state vector are taken independent and identically uniformly distributed in $[-1/2,1/2]$, and then the vector is normalized to unity.

[65] Bisection is the most efficient method to find zero of a monotonous function, $f(x)$, $x \in [a,b]$, $f(a) > 0 \& f(b) > 0$ as it minimizes number of evaluations of f needed to determine zero with a given accuracy; see L. I. Kronsjo, *Algorithms: Their Complexity and Efficiency* (John Wiley & Sons Ltd, London, 1979). Note the "float" nature of the algorithm illustrated with Fig. 1: Although it seems that the efficiency of the propagation between jumps (motion "up") can be increased by multiplying δt with $L > 2$ after every no-jump propagation step, this, in fact, will lower the efficiency of the zero determination (motion "down"). We could think of making up and down scalings different, by using different multipliers L; however, this will substantially complicate the algorithm.

[66] R. A. Horn and C. R. Johnson, *Norms for Vectors and Matrices* (Cambridge University Press, Cambridge, England, 1990).

[67] Definition of the Husimi distribution for model Eqs. (6) and (7) involves summation over series of binomial coefficients of the order N. It was not possible for us to go beyond $N = 2^{10} = 1024$ when calculating the corresponding Husimi distributions.

[68] A. Liniov, V. Volokitin, I. Meyerov, M. Ivanchenko, and S. Denisov, *Communications in Computer and Information*

Science, edited by V. Voevodin and S. Sobolev, Supercomputing RuSCDays 2017 (Springer-Verlag, New York, 2017), Vol. 793, pp. 136–150.

[69] H.-P. Breuer, E.-M. Laine, J. Piilo, and B. Vacchini, Rev. Mod. Phys. **88**, 021002 (2016).

[70] J. Piilo, S. Maniscalco, K. Härkönen, and K.-A. Suominen, Phys. Rev. Lett. **100**, 180402 (2008); J. Piilo, K. Härkönen, S. Maniscalco, and K.-A. Suominen, Phys. Rev. A **79**, 062112 (2009).

[71] A. A. Budini, Phys. Rev. A **88**, 012124 (2013).

[72] L. Magazzù, S. Denisov, and P. Hänggi, Phys. Rev. A **96**, 042103 (2017).

[73] J. P. Garrahan and I. Lesanovsky, Phys. Rev. Lett. **104**, 160601 (2010).

[74] E. M. Kessler, G. Giedke, A. Imamoglu, S. F. Yelin, M. D. Lukin, and J. I. Cirac, Phys. Rev. A **86**, 012116 (2012).

[75] P. E. Kloeden and E. Platen, *Numerical Solution of Stochastic Differential Equations* (Springer, Berlin, 1992).